NANO · MICRO small
www.small-journal.com

Parallel Fabrication of Self-Assembled Nanogaps for Molecular Electronic Devices

Johnas Eklöf-Österberg, Tina Gschneidtner, Behabitu Tebikachew, Samuel Lara-Avila, and Kasper Moth-Poulsen**

Single molecule electronics might be a way to add additional function to nanoscale devices and continue miniaturization beyond current state of the art. Here, a combined top-down and bottom-up strategy is employed to assemble single molecules onto prefabricated electrodes. Protodevices, which are self-assembled nanogaps composed by two gold nanoparticles linked by a single or a few molecules, are guided onto top-down prefabricated nano-sized nickel electrodes with sandwiched palladium layers. It is shown that an optimized geometry of multilayered metallic (top-down) electrodes facilitates the assembly of (bottom-up) nanostructures by surface charge interactions. Moreover, such assembly process results in an electrode–nanoparticle interface free from linking molecules that enable electrical measurements to probe electron transport properties of the nanoparticle–molecule–nanoparticle protodevices.

One route to continue downscaling of electronic components and to augment the functionality of electronic devices is single (or a few) molecule electronics.[1–3] Molecules are a factor of ten smaller in dimension than the smallest nodes of the transistors today and even smaller by volume, they can be synthesized in molar amounts and show promising properties such as photoswitching[4,5] and rectifying behavior.[6,7]

One of the major obstacles when constructing single molecule logic circuits is to position a single molecule in a nanogap enabling electronic characterization. Several experimental platforms have been developed, including mechanical break junction (MCBJ),[8–10] scanning probe microscopy (SPM),[11,12] electromigration break junction (EBJ),[13–15] surfactant-assisted parallel electroless plating,[16] and shadow mask evaporation,[17,18] and the field has recently been reviewed.[19,20] Meanwhile new parallel fabrication strategies for formation of nanogap electrodes are being developed, here recent examples include molecular crystal lithography,[21] gold nanorod alignment,[22] crack-defined electronic nanogaps,[23] self-limiting electrode growth,[24] the use of graphene-based constrictions,[25] and carbon nanotube electrodes.[26,27] A remaining challenge is scalability, that is, how to position single (or a few) molecules in the nanogap in a parallel way. In this context, an interesting approach is the use of the protodevice concept, where the single (or a few) molecule is isolated in the solution between nanoparticles, and subsequently self-assembled onto prefabricated nanoelectrodes.[28–34]

Templated self-assembly can be used to position nanoparticles at prefabricated surfaces. Examples include positioning of gold nanoparticles and orientation of gold nanorods.[35,36] It is also possible to assemble particles using a meniscus flow over nanostructures,[37,38] chemically activate and passivate parts of a surface prior to deposition of nanoparticles,[39] making use of variations of hydrophobicity on a surface[40] or wet-contact printing.[41] Other methods involve electrostatic trapping of particles attached with molecules.[42–44]

Here we explore the natural surface charges that different metal/metal oxides acquire in solution to guide bottom-up assembled molecular linked nanoparticle dimers to prefabricated electrodes (**Figure 1**). It is in this manner possible to position, isolate, and measure electron transport on a single (or a few) molecules. Electron-beam lithography (EBL) was used to fabricate electrode pairs, with optimized geometry and materials to promote the assembly of negatively charged nanoparticle dimers (**Figure 2**). The electrodes are made in layers of nickel (Ni) and palladium (Pd). Nickel has proven to be able to attract negatively charged citrate stabilized nanoparticles due to the positive surface potential at pH 6.5–7.[45] Pd is sandwiched between the Ni electrodes to improve the conductivity of the electrodes, and to enable an oxide free interface between the electrodes and protodevices. At the same time the top Pd layer reduces assembly of nanoparticles "on top" of the electrodes. Two different molecules, 1,6-hexanedithiol and 1,4-benzenedithiol, were used as test molecules for the construction of

J. Eklöf-Österberg, Dr. T. Gschneidtner, B. Tebikachew, Prof. K. Moth-Poulsen
Department of Chemistry and Chemical Engineering
Chalmers University of Technology
Gothenburg 412 96, Sweden
E-mail: johnas.eklof@chalmers.se; kasper.moth-poulsen@chalmers.se
Prof. S. Lara-Avila
Department of Microtechnology and Nanoscience
Chalmers University of Technology
Gothenburg 412 96, Sweden
Prof. S. Lara-Avila
National Physical Laboratory
Teddington TW11 0LW, UK
The ORCID identification number(s) for the author(s) of this article can be found under https://doi.org/10.1002/smll.201803471.

DOI: 10.1002/smll.201803471

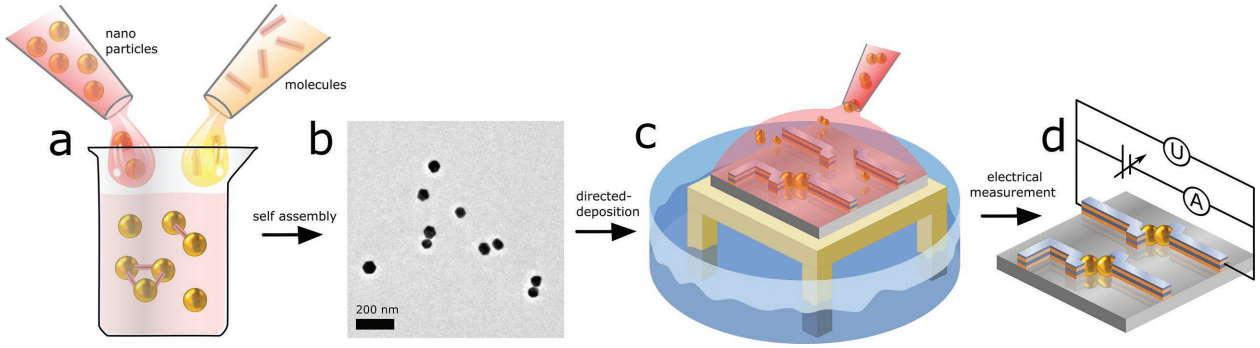

Figure 1. Fabrication scheme of two particles linked with one or a few molecules (protodevices). a) Self-assembly of a dispersion of 60 nm, citrate stabilized gold nanoparticles and molecular linkers (benzene 1,4-dithiol or 1,6-hexanedithiol) in solution. b) TEM microscopy image with single particles and dimers present. c) A mixture of the nanoparticle dispersion and 2-propanol (1:2) are applied to a chip with prefabricated nanosized electrodes. The chip is mounted on a specially designed, 3D printed scaffold placed in a petri dish filled with water and 2-propanol (1:2) and sealed with a glass lid. d) The chip was washed and dried, leaving dimeric structures in between the electrodes for electrical measurements.

nanoparticle dimer "protodevices" (**Figure 3**). In practice, the assembly took place inside an enclosure filled with a mixture of water and 2-propanol to saturate the atmosphere, preventing the droplet of dimer dispersion to dry before the end of the deposition.[46] Electric measurements were performed on devices where protodevices were successfully assembled.

We have combined bottom-up and top-down techniques for the construction of nanosized objects in which nanoparticle dimers, the so-called protodevices, assemble in water onto prefabricated electrodes. All dimers assembling to the electrodes carry a single or a few molecules, since the molecule is the reason that the dimer was formed in the first place in the dispersion. Such dimers were formed in solution by fine-tuning the amount of particles and molecular linkers. This assembly method yields 64% single particles, 24% dimers, 9% trimers, and 3% higher number cluster as shown in Figure 3.

A variety of deposition parameters was optimized in order to maximize the number of correctly deposited dimers in the nanogap electrodes. The nanoparticle dimer dispersion was mixed with 2-propanol in order to fine-tune the polarity of the solution and by that increase the interactions between the positively charged nanoelectrodes and the negatively charged nanoparticles. The atmosphere around the Si/SiO_2 substrate was saturated by enclosing the chip inside a petri dish filled with a mixture of water and 2-propanol, using the same proportions as in the dispersion, preventing the droplet from drying out (Figure 1c). The outcome of the deposition was sensitive to 2-propanol, adding too much resulted in clusters covering the surface, no particles was assembled without the use of 2-propanol. Reaction time was also optimized in order to increase the number of successful depositions without increasing the number of clusters.

An initial focus point was the directed assembly of isolated nanoparticles onto prefabricated nanogaps. Various electrode geometries were explored as to optimize yields of self-assembled nanoparticles (**Figure 4**). These experiments shows that it is possible to fill 40% of the nanogaps in the array with a single or a few nanoparticles in the active part of the device. The successfully filled nanogaps are highlighted in blue and the successfully deposited nanoparticles in red.

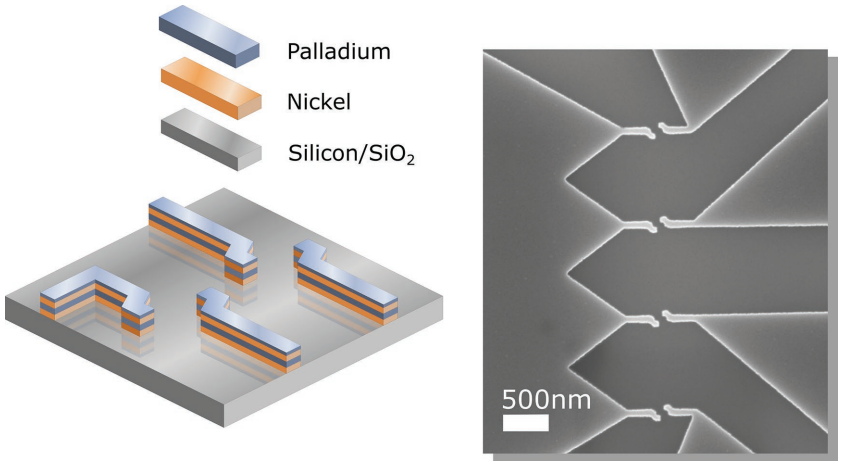

Figure 2. Schematic overview over the top-down fabricated electrodes, seen to the left, consisting of layers in the following order: Ni, Pd, Ni, Pd. An SEM microscopy image can be seen to the right in the figure. Ni in the electrodes is used to attract the negatively charged nanoparticles and the Pd layers are used both to increase conductivity and also to protect the top side of the electrodes from particle assembly.

A variety of geometrical structures and varying deposition times were made prior to the results in this work. The structures which were best at capturing nanoparticles, from those experiments, were used as an inspiration when designing the electrodes seen in Figure 6. Scanning electron microscope (SEM) microscopy images of this can be seen in the Supporting Information, Figures S1–S6.

The controlled design and fabrication of the electrodes allows us to maximize the assembly yield for either single particles or dimeric structures. SEM microscopy images in **Figure 5**a show an example of a design optimized to capture single nanoparticles. In Figure 5b, 25 out of 70 nanogaps had a single nanoparticle positioned in them, corresponding to 36%. The gap could be increased in order to be able to capture dimers (Figure 5c,d). A schematic is included

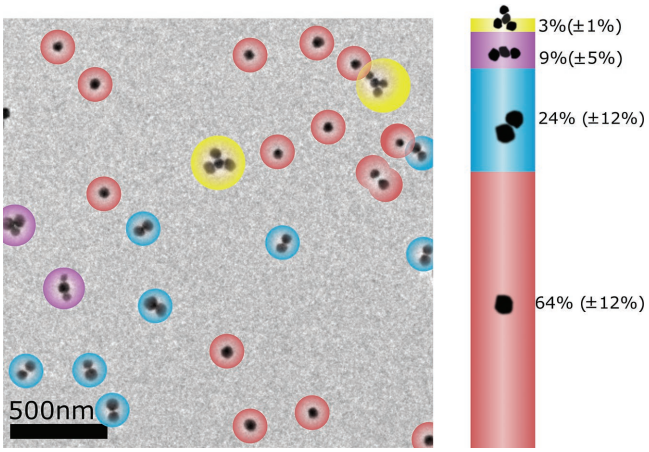

Figure 3. Representative TEM image of the nanoparticle dispersion upon addition of dithiol molecules, benzene 1,4-dithiol or 1,6-hexanedithiol. The TEM grid is treated with poly-L-lysine HBr to suppress agglomeration during the deposition, single particles are marked with red, dimers with blue, trimers with purple, and multimers with yellow. Stacked bar chart corresponds to benzene 1,4-dithiol with 64(±12)% singles, 24(±12)% dimers, 9(±5)% trimers, and 3(±1)%. Nanoparticles linked with 1,6-hexanedithiol were calculated to 67(±5)% singles, 21(±4)% dimers, 9(±3)% trimers, and 4(±2)% multimers.

in Figure 5e where two different electrode pairs are depicted. One with two contact arms marked in red and one pair with only one contact arm, the length of these can be varied in dimension *x*, see Figure 5e. A contact arm is used to maximize the contact area between electrode and particle, and in this way, minimize the contact resistance. In the end, shorter single arms as seen in Figure 5c,d were used leading to a capture of a single particle in 22 out of 70 devices, corresponding to 31%. It is noteworthy that in devices where the electrodes are fabricated entirely of Ni (Figure 5a,b and f), the assembly of particles occurs not only in the gap between electrodes but also on top of them. Moreover, we have noticed that while the electrodes solely made of Ni lead to assembly of particles, the resulting electrical contacts to citrate stabilized particles are poor. We attribute this to the formation of a nickel oxide layer, either in ambient or in solution during particle assembly, that prevents good electric contact to the Au nanoparticles.

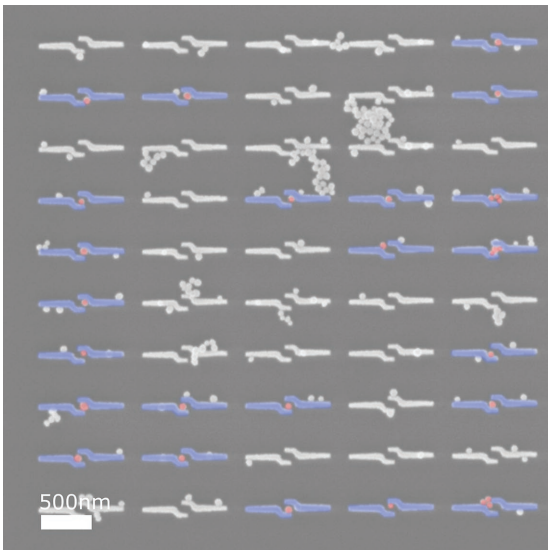

Figure 4. SEM microscopy image of a part of an array of Ni nanogaps after deposition of nanoparticles. Successfully placed particles are highlighted as red. 40% of the nanogaps had a successful deposition (highlighted in blue).

In order to maximize the capture of nanoparticle dimers, the contact was modified by increasing the gap size from 60 nm as seen in Figure 5a to 130–140 nm as seen in Figure 5c,d. The additional 10–20 nm spacing between the electrode pairs was added due to the hydrodynamic diameter (74 nm) of the particles plus the size distribution, measured in previous work by Eklöf et al.[45] In addition, the prefabricated contacts consist of stacked Ni-Pd, with Ni to promote the particle assembly and Pd as the top-most layer to reduce the amount of nanoparticles attached to the top of the electrodes. Two possible geometries of dimers' sitting between an electrode pair can be seen in Figure 5c,d. In terms of electrical measurements, the protodevice of Figure 5c forms an ideally assembled structure, in which each Au nanoparticle is in contact with a prefabricated electrode; from a chip with 60 nanogaps, two to three functional devices could be assembled and measured.

As a proof of concept, electrical characterization was performed (two-contact resistance) on devices where assembly of protodevices results in each Au nanoparticle seemingly contacting a prefabricated electrode (**Figure 6**a, see also Figure 5c). The red line in Figure 6b shows a typical IV curve through a dimer protodevice linked with benzene 1,4-dithiol marked as red and 1,6-hexanedithiol as blue. The black line is an electrode pair without any particle attached to it. The resistance through the nanoparticle dimer with either benzene 1,4-dithiol or 1,6-hexanedithiol is significantly lower compared to the empty electrode pair, showing that the protodevices conduct.

The protodevice assembly here demonstrated by SEM and electrical measurements could be used as metallic nanogaps for molecule assembly. Overall, for nanoparticle dimer assembly we obtain a yield of 4% for both dimers linked with 1,6-hexanedithiol or benzene 1,4-dithiol. We believe that this number would be higher if for instance if the percentage of dimers in the dispersion (Figure 3) was larger. Higher concentrations of dimers are definitely possible to achieve using elaborate synthesis and purification solutions, however, these are not used in the work at hand due to the complexity.[29,39,47,48] Another consideration is that dimers may cluster in the deposition progress either due to the 2-propanol mixture, residues on the surface, or other unknown parameters affecting the deposition negatively.

This work shows that it is possible to isolate, position, and electrically contact bottom-up assembled nanoparticle dimers linked with a single or a few molecules in a parallel way onto top-down fabricated nanosized electrodes. We have assembled gold nanoparticles linked with 1,6-hexanedithiol or benzene 1,4-dithiol in dispersion and assembled them onto prefabricated nanosized electrodes placed on a Si/SiO_2 chip, specially designed to attract negatively charged nanoparticle dimers. The electrodes were made out of Ni with Pd layers sandwiched between the Ni layers. It was known from previous work[45] and from prestudies presented in this article that Ni attracts negatively charged nanoparticles and that it is possible

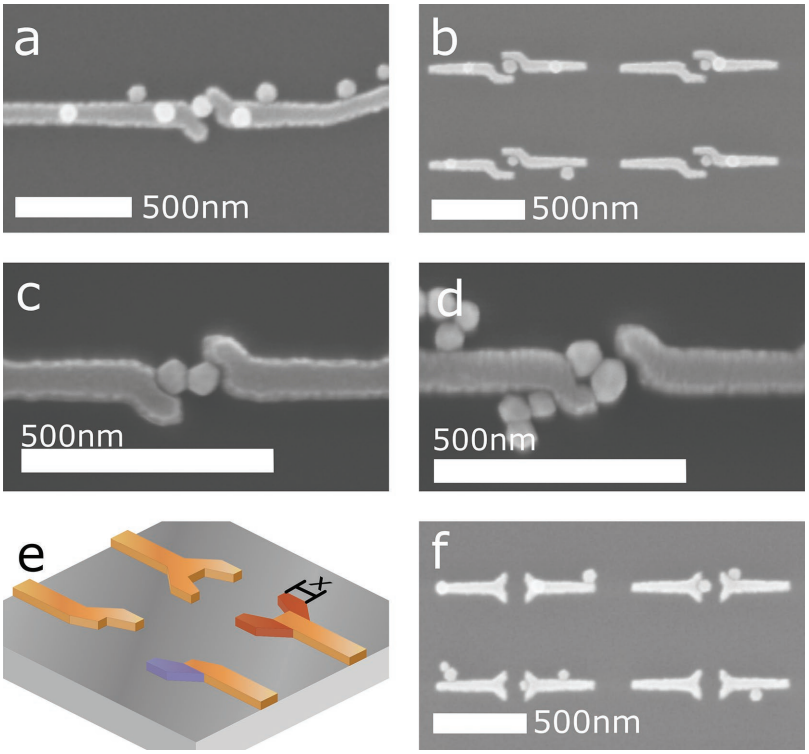

Figure 5. Scanning electron microscope (SEM) images of assembly on prefabricated nanogaps. a) A pair of nickel electrodes (70 nm thick), designed to capture single nanoparticles. b,f) Successfully assembled single particles, in an array of nickel-nanogap. The contact arms in (b) will cause short circuit when depositing dimers. c) An ideal placed dimer, with connection between the particles and the electrodes. d) The dimer is, in this device, only attached to one of the electrodes, hampering electrical measurement. The electrodes in (c) and (d) are shorter compared to (b) to prevent short circuit. e) a schematic over the electrodes, highlighting the contact arms.

to fill up to 40% of Ni nanogaps in an array with single nanoparticles, however, solid Ni electrodes had a poor conductance. Pd was therefore sandwiched into the Ni electrodes to improve the conductance of the electrodes. A top layer of Pd was added to protect the top surface from deposition of nanoparticle dimers. The electrodes were fabricated using electron-beam lithography, however, due to the final design this technique can be exchanged with conventional UV-lithography, which means that nanogaps containing a single or a few active molecules can in essence be realized without any high end nanofabrication tools. The dimers were investigated using transmission electron microscope (TEM) prior to deposition in order to determine the percentage of dimers present (24%) in the nanoparticle dispersion. It was found via SEM that two to three of the electrode pairs were filled with a dimer particle after deposition on one chip with 60 nanogaps present. Electrical measurements were used as a proof of concept that the dimers are conducting. The yield of successful depositions of dimers is still low, we envision that the yield can be improved by changing from Si/SiO_2 to another substrate or by optimizing the synthesis of nanoparticle dimers, using more elaborate synthetic approaches.[29,39,47,48] Moreover, we envision that in this way combined top-down–bottom-up "strategies" can be used to fabricate complex nanostructures not attainable by conventional techniques in a parallel way.

Experimental Section

Preparation of Nanosized Electrodes: Nanosized electrodes were fabricated on a conductive, P-doped, 3″ Si/SiO2 wafer (1–10 Ωcm) by combining photo- and electron-beam lithography. Small features were fabricated with electron-beam lithography (EBL-JEOL JBX 9300FS at 100kV) using a bilayer lift-off resist system, consisting of a 100 nm thick bottom layer (MCC NANO Copolymer EL6, Microlithography Chemicals Corp.) followed by a 50 nm thick top layer (ARP 6200.13:Anisol 1:2, Allresist GmBH). Palladium (Pd) and nickel (Ni) were used at metallization layers (Lesker PVD 225) in the following order and thickness: 20 nm Ni, 20 nm Pd, 20 nm Ni, and 3 nm Pd.

The larger parts of the electrodes were fabricated using a direct laser writer (l = 405 nm, Heidelberg Instruments DWL 2000) and a bilayer resist composed of LOR3A (Microlithography Chemicals Corp.) as bottom layer and S1813 resist (Microresist GmBH) as top layer. For metallization of large contacts, Pd (3 nm)/Ti (5 nm)/Au (100 nm) were used. After wafer dicing, the final step before assembly of protodevices was a cleaning step in O2-plasma for 1 min at 50 W. In total, every chip contained 60 devices. A schematic depicting the electrode design and an SEM microscopy image before any particle deposition can be seen in Figure 2.

Synthesis of Nanoparticle Dimers: All solvents were used without further purification. 1,6-Hexanedithiol (97%) and benzene 1,4-dithiol (98%) were purchased from Alfa Aesar and spherical citrate stabilized gold nanoparticles 60 nm were purchased from Sigma-Aldrich. Particles in this size are relatively simple to distinguish using dark field microscopes or SEM. It is also simple to fabricate the needed nanogaps in the size range of 60–140 nm using more conventional techniques such as UV-lithography.

The dimeric nanoparticles were prepared by tuning the amount of molecular linker in between the particles to achieve a good amount of dimeric particles, in a yield of around 24%.

The purchased nanoparticle (NP) solution (1.9×10^{10} NP mL^{-1}) was first concentrated ten times and the amount of citrate stabilizers reduced by the factor of 33, by centrifugation. A high density of citrate prevents the NPs to get into close contact and therefore less dimeric structures are observed. The final volume of colloidal NPs is 100 µL.

To 100 µL of NP solution, 5 µL of a 3×10^{-6} M dithiol linker solution was added, 1,6-hexanedithiol and benzene 1,4-dithiol were both dissolved in ethanol (0.01 M) prior dilution in water to 3×10^{-6} M.

The NP-linker solution was left for 16 h on a rocking table and then used without further purification for the deposition.

The dimers were characterized with a TEM (Tecnai T20 LaB6). A carbon-layered TEM grid was prefunctionalized with poly-L-lysine hydrobromide to prevent agglomeration of the negatively charged nanoparticles. With this method, citrate stabilized NPs are spread all over the TEM grid. Aggregation of the nanoparticles on the TEM sample is thus minimal.

Deposition of NP Dimers onto Electrodes: As visualized in the schematic of Figure 1c,d. The chip was mounted on a 3D printed scaffold placed in a petri dish filled with a 1:2 water:2-propanol mixture. A 4 µL drop of NP dimers and 2-propanol was added on the chip and kept there for 2 d before rinsing the chip in deionized water and drying it with N_2 gas.

Characterization of Deposited NPs: An SEM (Zeiss Supra 60 VP), with an accelerating voltage of 5 kV and a background pressure of 5×10^{-7} mbar was used to quickly investigate the samples before electrical measurement in order to detect electrode pairs with attached nanoparticle dimers. SEM images were captured with the same SEM

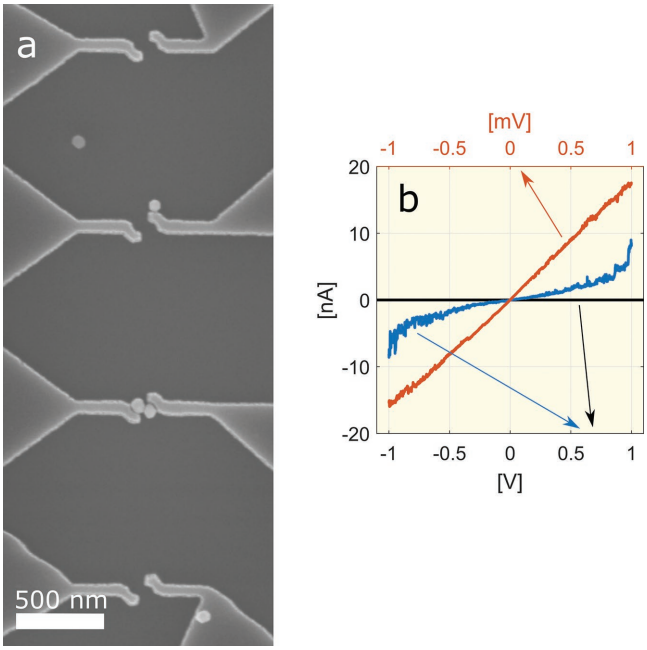

Figure 6. Electrical characterization of assembled protodevices. a) SEM image is used to identify devices suitable for electrical characterization. b) Current–voltage (*I*–*V*) characteristic of prefabricated electrodes with no nanoparticle dimer present (black), dimer nanoparticles linked with benzene 1,4-dithiol (red), and dimer linked with 1,6-hexanedithiol as blue.

as the quick inspection, using the In-lens detector and an aperture of 30 µm, the only difference was the acceleration voltage which was in this case set to 10 kV. A 30 µm aperture and the In-lens detector were used when capturing the SEM images.

The electrical two-point measurement was performed using a probe station (Keithley 4200-SCS) equipped with four Source Measure Units (SMUs) connected to a Karl Suss PM5 probe station with six probe heads. The current compliance was set to 100 nA and the voltage compliance was set between 2 and 20 V depending on the measurement. A reference measurement was performed on a wire manufactured in the same way as the electrical contacts to ensure a good electrical interface between large and small contacts fabricated in different lithography steps.

Supporting Information

Supporting Information is available from the Wiley Online Library or from the author.

Acknowledgements

This work was supported by the Myfab National Access program (at MC2 Nano Fabrication Laboratory, Chalmers), the Knut and Alice Wallenberg Foundation, Chalmers Area of Advance Nano, and the European Research Council (ERC).

Conflict of Interest

The authors declare no conflict of interest.

Keywords

molecular electronics, nanofabrication, self-assembly

Received: August 27, 2018
Revised: October 4, 2018
Published online:

[1] A. Aviram, M. A. Ratner, *Chem. Phys. Lett.* **1974**, *29*, 277.
[2] L. A. Bumm, J. J. Arnold, M. T. Cygan, T. D. Dunbar, T. P. Burgin, L. J. Ii, D. L. Allara, J. M. Tour, P. S. Weiss, *Science* **1996**, *271*, 1705.
[3] N. Xin, X. Guo, *Chem* **2017**, *3*, 373.
[4] M. Zhuang, M. Ernzerhof, *Phys. Rev. B* **2005**, *72*, 073104.
[5] C. Jia, A. Migliore, N. Xin, S. Huang, J. Wang, Q. Yang, S. Wang, H. Chen, D. Wang, B. Feng, Z. Liu, G. Zhang, D.-H. Qu, H. Tian, M. A. Ratner, H. Q. Xu, A. Nitzan, X. Guo, *Science* **2016**, *352*, 1443.
[6] B. Capozzi, J. Xia, O. Adak, E. J. Dell, Z.-F. Liu, J. C. Taylor, J. B. Neaton, L. M. Campos, L. Venkataraman, *Nat. Nanotechnol.* **2015**, *10*, 522.
[7] J. Trasobares, D. Vuillaume, D. Théron, N. Clément, *Nat. Commun.* **2016**, *7*, 12850.
[8] M. A. Reed, C. Zhou, C. J. Muller, T. P. Burgin, J. M. Tour, *Science* **1997**, *278*, 252.
[9] M. Kiguchi, S. Kaneko, *Phys. Chem. Chem. Phys.* **2013**, *15*, 2253.
[10] N. Muthusubramanian, E. Galan, C. Maity, R. Eelkema, F. C. Grozema, H. S. J. van der Zant, *Appl. Phys. Lett.* **2016**, *109*, 013102.
[11] G. Binnig, C. F. Quate, *Phys. Rev. Lett.* **1986**, *56*, 930.
[12] X. Hao, N. Zhu, T. Gschneidtner, E. Ö. Jonsson, J. Zhang, K. Moth-Poulsen, H. Wang, K. S. Thygesen, K. W. Jacobsen, J. Ulstrup, Q. Chi, *Nat. Commun.* **2013**, *4*, 2121.
[13] H. S. J. van der Zant, E. A. Osorio, M. Poot, K. O. Kavli, *Phys. Status Solidi B* **2006**, *243*, 3408.
[14] H. B. Heersche, G. Lientschnig, K. O'Neill, H. S. J. van der Zant, H. W. Zandbergen, *Appl. Phys. Lett.* **2007**, *91*, 072107.
[15] H. Park, A. K. L. Lim, A. P. Alivisatos, J. Park, P. L. McEuen, *Appl. Phys. Lett.* **1999**, *75*, 301.
[16] V. M. Serdio V, T. Muraki, S. Takeshita, D. E. Hurtado S, S. Kano, T. Teranishi, Y. Majima, *RSC Adv.* **2015**, *5*, 22160.
[17] S. Kubatkin, A. Danilov, M. Hjort, J. Cornil, J.-L. Brédas, N. Stuhr-Hansen, P. Hedegård, T. Bjørnholm, *Nature* **2003**, *425*, 698.
[18] M. Kölbel, R. W. Tjerkstra, J. Brugger, C. J. M. Van Rijn, W. Nijdam, J. Huskens, D. N. Reinhoudt, *Nano Lett.* **2002**, *2*, 1339.
[19] L. Sun, Y. A. Diaz-Fernandez, T. A. Gschneidtner, F. Westerlund, S. Lara-Avila, K. Moth-Poulsen, *Chem. Soc. Rev.* **2014**, *43*, 7378.
[20] D. Xiang, X. Wang, C. Jia, T. Lee, X. Guo, *Chem. Rev.* **2016**, *116*, 4318.
[21] L. Jiang, H. Dong, Q. Meng, J. Tan, W. Jiang, C. Xu, Z. Wang, W. Hu, *Adv. Mater.* **2012**, *24*, 694.
[22] T. Jain, S. Lara-Avila, Y.-V. Kervennic, K. Moth-Poulsen, K. Nørgaard, S. Kubatkin, T. Bjørnholm, *ACS Nano* **2012**, *6*, 3861.
[23] V. Dubois, F. Niklaus, G. Stemme, *Adv. Mater.* **2016**, *28*, 2178.
[24] Y. Majima, G. Hackenberger, Y. Azuma, S. Kano, K. Matsuzaki, T. Susaki, M. Sakamoto, T. Teranishi, *Sci. Technol. Adv. Mater.* **2017**, *18*, 374.
[25] C. Jia, A. Migliore, N. Xin, S. Huang, J. Wang, Q. Yang, S. Wang, H. Chen, D. Wang, B. Feng, Z. Liu, G. Zhang, D.-H. Qu, H. Tian, M. A. Ratner, H. Q. Xu, A. Nitzan, X. Guo, *Science* **2016**, *352*, 1443.
[26] Q. Xu, G. Scuri, P. Mathewson Carly, Kim, C. Nuckolls, B. Delphine, *Nano Lett.* **2017**, *17*, 5335.
[27] J. Zhu, J. McMorrow, R. Crespo-Otero, G. Ao, M. Zheng, W. Gillin, M. Palma, *J. Am. Chem. Soc.* **2016**, *138*, 2905.

[28] T. Dadosh, Y. Gordin, R. Krahne, I. Khivrich, D. Mahalu, V. Frydman, J. Sperling, A. Yacoby, I. Bar-Joseph, *Nature* **2005**, *436*, 677.
[29] Y. D. Fernandez, L. Sun, T. Gschneidtner, K. Moth-Poulsen, *APL Mater.* **2014**, *2*, 010702.
[30] T. A. Gschneidtner, Y. A. Diaz Fernandez, K. Moth-Poulsen, *J. Mater. Chem. C* **2013**, *1*, 7127.
[31] M. R. Dewi, T. A. Gschneidtner, S. Elmas, M. Ranford, K. Moth-Poulsen, T. Nann, *ACS Nano* **2015**, *9*, 1434.
[32] T. Jain, Q. Tang, T. Bjørnholm, K. Nørgaard, *Acc. Chem. Res.* **2014**, *47*, 2.
[33] S. Kano, K. Maeda, D. Tanaka, M. Sakamoto, T. Teranishi, Y. Majima, *J. Appl. Phys.* **2015**, *118*, 134304.
[34] K. S. Makarenko, Z. Liu, M. P. de Jong, F. A. Zwanenburg, J. Huskens, W. G. van der Wiel, *Adv. Mater.* **2017**, *29*, 1702920.
[35] V. Flauraud, M. Mastrangeli, G. D. Bernasconi, J. Butet, D. T. L. Alexander, E. Shahrabi, O. J. F. Martin, J. Brugger, *Nat. Nanotechnol.* **2017**, *12*, 73.
[36] C. Kuemin, L. Nowack, L. Bozano, N. D. Spencer, H. Wolf, *Adv. Funct. Mater.* **2012**, *22*, 702.
[37] S. Ni, M. J. K. Klein, N. D. Spencer, H. Wolf, *Langmuir* **2014**, *30*, 90.
[38] S. Ni, J. Leemann, I. Buttinoni, L. Isa, H. Wolf, *Sci. Adv.* **2016**, *2*, e1501779.
[39] Y. A. Diaz Fernandez, T. A. Gschneidtner, C. Wadell, L. H. Fornander, S. Lara Avila, C. Langhammer, F. Westerlund, K. Moth-Poulsen, *Nanoscale* **2014**, *6*, 14605.
[40] N. K. Mandsberg, O. Hansen, R. Taboryski, *Sci. Rep.* **2017**, *7*, 12794.
[41] M. Mayer, M. Tebbe, C. Kuttner, M. J. Schnepf, T. A. Koenig, A. Fery, *Faraday Discuss.* **2016**, *191*, 159.
[42] Y. Yu, X. Chen, Y. Wei, J.-H. Liu, S.-H. Yu, X.-J. Huang, *Small* **2012**, *8*, 3274.
[43] S. H. M. Jafri, H. Löfås, T. Blom, A. Wallner, A. Grigoriev, R. Ahuja, H. Ottosson, K. Leifer, *Sci. Rep.* **2015**, *5*, 14431.
[44] S. H. M. Jafri, T. Blom, K. Leifer, M. Strømme, H. Lövås, A. Grigoriev, R. Ahuja, K. Welch, *Nanotechnology* **2010**, *21*, 435204.
[45] J. Eklöf, A. Stolaś, M. Herzberg, A. Pekkari, B. Tebikachew, T. Gschneidtner, S. Lara-Avila, T. Hassenkam, K. Moth-Poulsen, *EPL* **2017**, *119*, 18004.
[46] J. Eklöf, T. Gschneidtner, S. Lara-Avila, K. Nygård, K. Moth-Poulsen, *RSC Adv.* **2016**, *6*, 104246.
[47] T. Lahtinen, E. Hulkko, K. Sokolowska, T.-R. Tero, V. Saarnio, J. Lindgren, M. Pettersson, H. Hakkinen, L. Lehtovaara, *Nanoscale* **2016**, *8*, 18665.
[48] K. Sokolowska, E. Hulkko, L. Lehtovaara, T. Lahtinen, *J. Phys. Chem. C* **2018**, *122*, 12524.